Journal of Alloys and Compounds 492 (2010) 373–377

Contents lists available at ScienceDirect

Journal of Alloys and Compounds

journal homepage: www.elsevier.com/locate/jallcom

Characterization of microstructures obtained in wedge shaped Al–Zn–Mg ingots

M.A. Suarez[a,*], O. Alvarez[a], M.A. Alvarez[a], R.A. Rodriguez[b], S. Valdez[c], J.A. Juarez[a]

[a] Instituto de Investigaciones en Materiales, Universidad Nacional Autónoma de México, Circuito Exterior S/N, Cd. Universitaria, C.P. 04510, Mexico D.F., Mexico
[b] Facultad de Química, Universidad Nacional Autónoma de México, Circuito Exterior S/N, Cd. Universitaria, C.P. 04510, Mexico D.F., Mexico
[c] Instituto de Ciencias Físicas, Universidad Nacional Autónoma de México (UNAM), Av. Universidad S/N, Col. Chamilpa, Cuernavaca, C.P. 62210, Morelos, Mexico

ARTICLE INFO

Article history:
Received 8 September 2009
Received in revised form
11 November 2009
Accepted 17 November 2009
Available online 20 November 2009

Keywords:
Aluminum alloy
Solidification
Microstructure
Approximant
Electrochemical efficiency

ABSTRACT

The structure present in chill casting taper section of Al–5.3at.%Zn + Mg additions between 3 and 40at.%Mg have been studied by scanning electron microscopy, microanalysis and X-ray diffractometry in order to relate the impact of intermetallic phases such as the τ-$Mg_{32}(Al,Zn)_{49}$ obtained at low Mg-contents with an approximant phase related to quasicrystals at high Mg-contents on its electrochemical efficiency. After microstructural and electrochemical efficiency characterization, it was found that an alloy composition of Al–5.3at.%Zn–10at.%Mg showed a microstructure which consisted of α-Al dendrites with τ-phase precipitates showing an electrochemical efficiency of 90% fulfilling the needs for cathodic protection application of structural steels in sea water.

1. Introduction

The Al–Mg–Zn alloy system has a relatively complex equilibrium diagram. The first investigation of the entire system was carried out by Eger in 1913[1]. Ever since, a great amount of studies have been carried out due to its excellent mechanical properties reached after age hardening [2,3] and for the combination of low density and high strength, which have made of the Al-alloys the primary material, to be used in the aircraft and automotive industries.

Recently, the most commonly studied metals for cathodic protection systems have been alloys of magnesium, zinc and aluminium [4,5]. The low electrode potentials of Al-anodes are readily adaptable to a variety of saline environments such as sea water. Pure Al reaches a relatively noble solution potential in a saline medium as a result of its protective oxide film. The oxide is the cause of a rapid polarization when aluminium is placed under a corrosion load in a cathodic protection circuit. Nevertheless, the success of the Al-anode depends upon the alloying of certain metals whose surface role is to ultimately prevent the formation of a continuous adherent and protective oxide film on the alloy, thus, permitting continuous galvanic activity of the aluminium [6].

The Al–Zn–Mg system has been pointed out as a potential candidate to be used as an alloy for cathodic protection of extructures exposed to marine environments with special attention in the microstructures and the distribution of $(Al,Zn)_{49}Mg_{32}$ phase in the α-Al matrix, to promote a good surface activation of the anode, avoiding the formation of the continuous, adherent and protective oxide film on the alloy surface once in service [7–9]. For instance, the dispersion of the τ phase in the matrix can be increased by

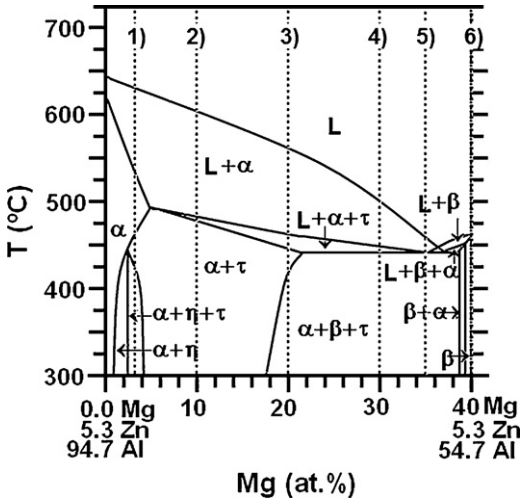

Fig. 1. Vertical section at constant 5.3at.%Zn of the ternary Al–Zn–Mg phase diagram [11]. The vertical broken lines show the Mg-content added to Al–5.3at.%Zn master alloy.

* Corresponding author. Tel.: +52 56 22 54 89; fax: +52 56 16 13 61.
E-mail address: msuarez@iim.unam.mx (M.A. Suarez).

0925-8388/$ – see front matter © 2009 Elsevier B.V. All rights reserved.
doi:10.1016/j.jallcom.2009.11.106

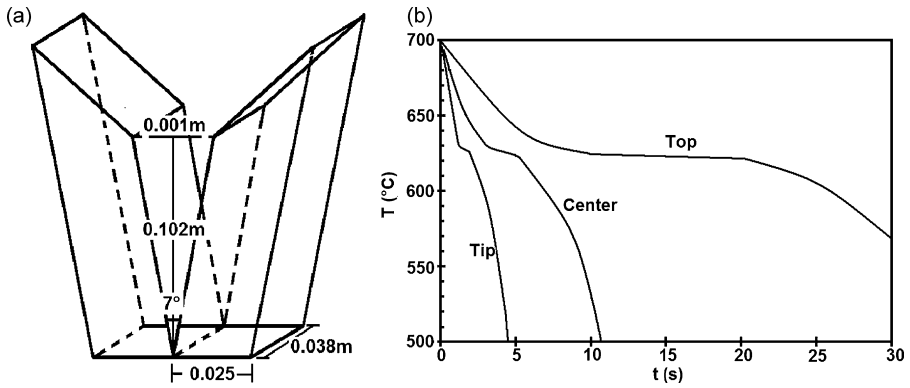

Fig. 2. (a) Dimensions of wedge shaped ingot used for gravity chill casting of Al–Zn–Mg alloys, (b) cooling curves obtained during solidification of Al–5.3at.%Zn–3at.%Mg. Top, center and tip correspond to thermocouple positions.

means of thermal treatments applied to as-cast ingots, by taking advantage of the fast kinetic reactions occurring in solid state at 400 °C, giving as a result Al-anodes with electrochemical efficiencies up to 78% [10].

The purpose of this work is to present the results of the microstructural characterization of wedge shaped ingots of Al–5.3at.%Zn master alloy with additions of Mg and to find the Mg content which promotes a good surface activation of the Al–Zn–Mg alloy to make possible its application as aluminium sacrificial anode.

2. Experimental procedures

Different alloys Al–5.3at.%Zn with Mg additions of 3, 10, 20, 30, 35 and 40at.% were made by induction melting of high purity (99.99at.%) elements in alumina crucibles. The compositions are shown in the phase diagram by vertical broken lines (Fig. 1) [11].

In all the experiments the alloys were cast at 75 K superheat above the liquidus temperature into a wedge shaped copper mould (Fig. 2(a)). During the experiments three thermocouples type K were introduced through the side of the mould and were located centrally at 20, 50 and 70 mm from tip to top of the mould cavity and the outputs were recorded on a Electroservoscribe chart recorder indicating cooling rates of 150, 50 and 20 K/s, for the lower, middle and upper thermocouple positions, respec-

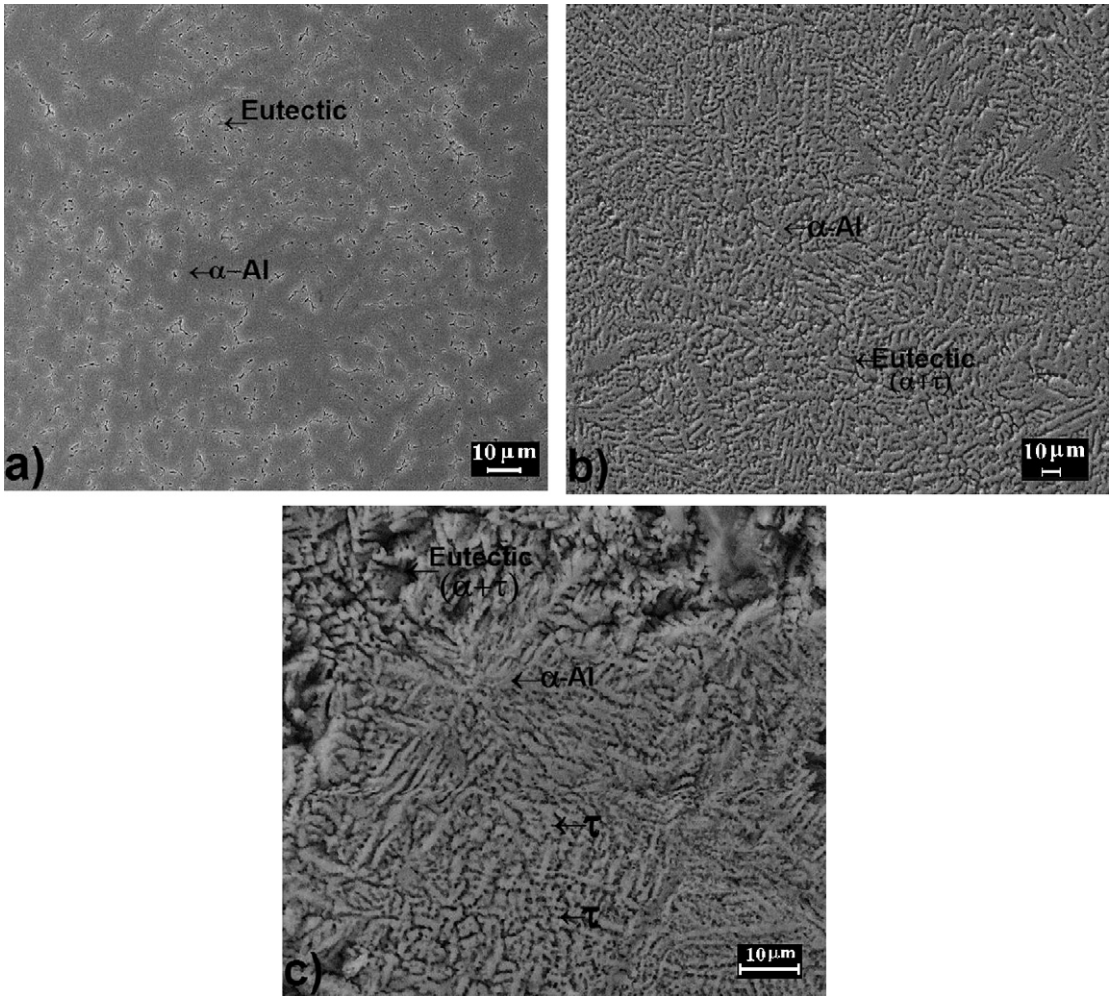

Fig. 3. Microstructure observed in wedge shaped ingot of Al–5.3at.%Zn–10at.%Mg. (a) Tip, (b) center and (c) top area of ingot. Gray and black areas correspond to the α-Al solid solution and the eutectic α+τ, respectively.

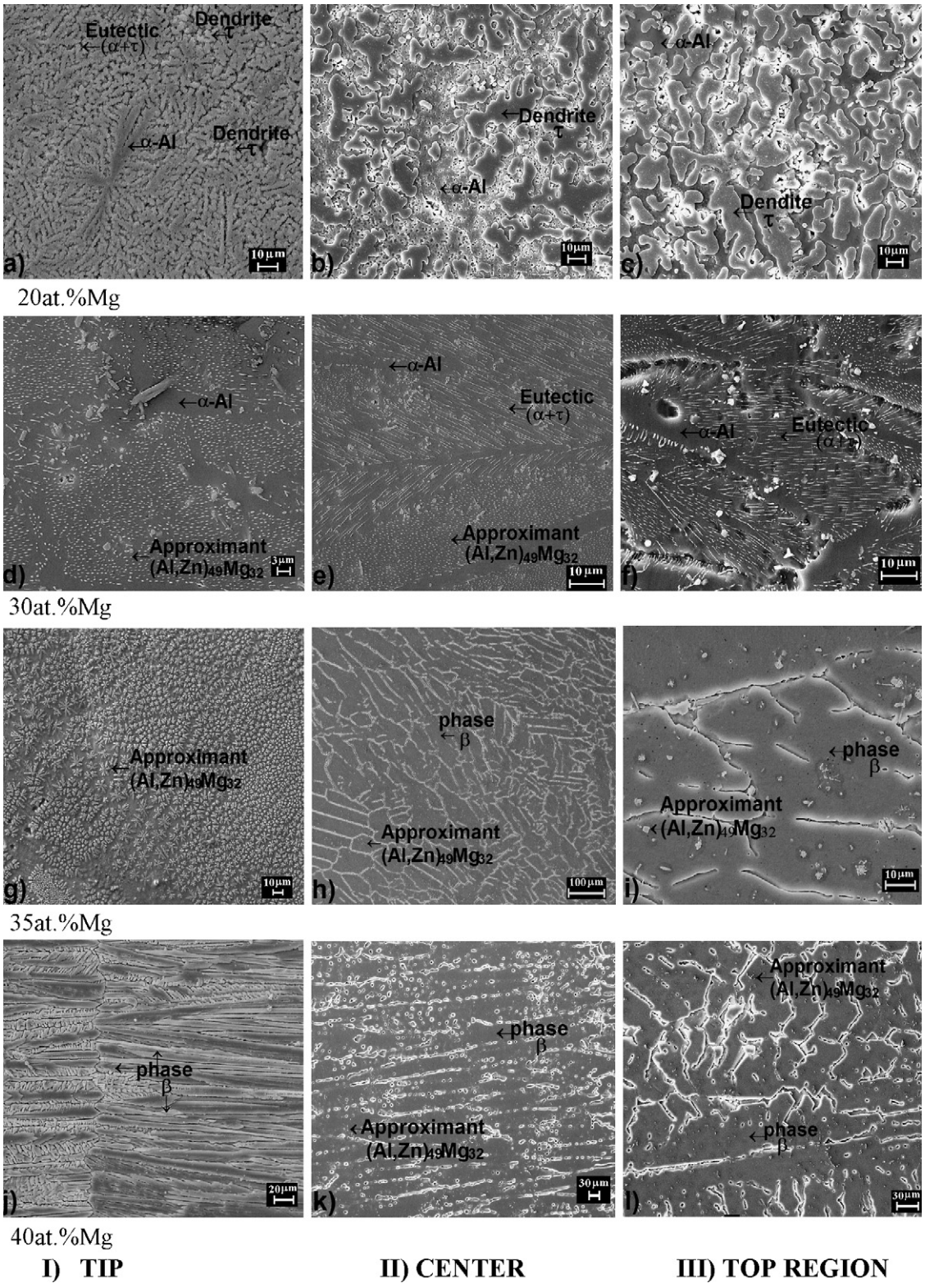

Fig. 4. Microstructures observed in Al–Zn–Mg wedge shaped ingots. (I) Tip, (II) center, (III) top region.

tively (Fig. 2(b)). Ingots were sectioned longitudinally and centrally to the plane normal to the diverging wedge faces, polished and etched with Keller's reagent in order to reveal the microstructure. The regions of characteristic morphology were located by scanning electronic microscopy (Stereoscan 440). X-ray diffractometry was performed by using a diffractometer Siemens 5000 with Cu Kα radiation ($\lambda = 1.5418$ Å) with a scanning speed of 1°/min and a scanning angle of 10–120°.

The electrochemical behavior of Al–5.3at.%Zn–xat.%Mg alloys was investigated in 3% NaCl solution. The electrochemical tests were carried out in a three-cell arrangement. The samples of the Al-anode were put in a sample holder presenting an exposed area of 120 mm^2 to the electrolyte. A platinum gauge was used as a counter electrode and a saturated calomel electrode was employed as a reference electrode.

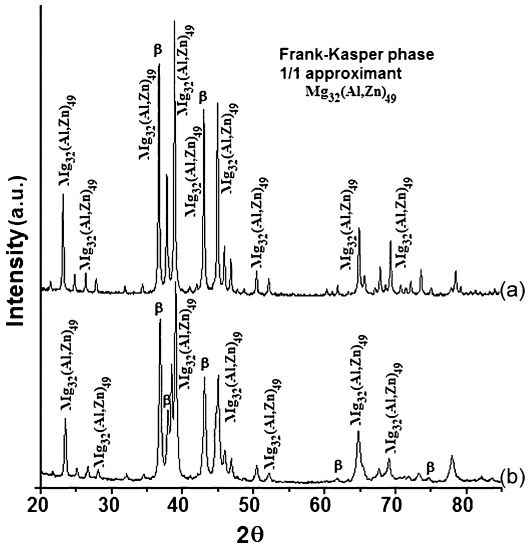

Fig. 5. Powder diffraction for the 1/1 crystalline approximant to icosahedral Al–Zn–Mg alloy. X-ray diffraction patterns of Al–5.3at.%Zn–35at.%Mg obtained in (a) the tip and (b) center of ingot.

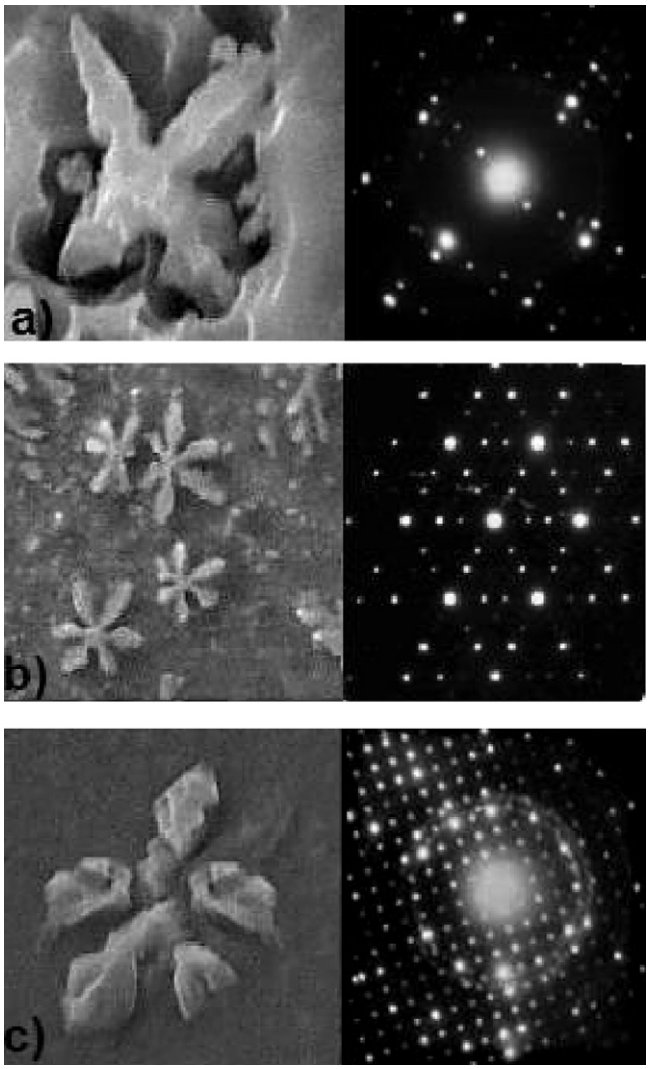

Fig. 6. (a) Two, (b) three and (c) fivefold morphology and their diffraction patterns of the approximant to quasicrystal observed in tip region of Al–5.3at.%Zn–35at.%Mg ingots.

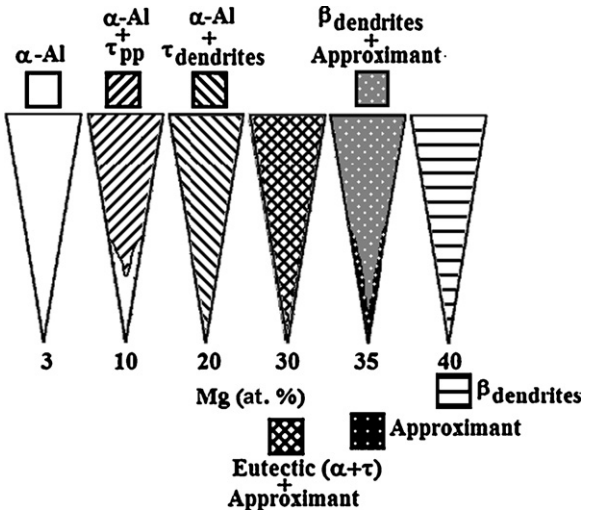

Fig. 7. Location of structure zone in chill-cast wedges of Al–5.3at.%Zn with additions of Mg.

3. Results and discussion

3.1. Microstructural characterization

Depending on cooling rate and Mg content, the Al–5.3at.%Zn–xat.%Mg alloys present different microstructures and are as follow:

The microstructures of Al–5.3at.%Zn–3at.%Mg alloy showed the presence of cellular α-Al solid solution with interdendritic eutectic in the three regions of ingot; tip, center and top area. The Al–5.3at.%Zn–10at.%Mg ingot showed in the tip dendrites of α-Al solid solution with eutectic (α+τ) in interdendritic regions while in center and top regions of the ingot, it was observed the presence of dendrites of α-Al solid solution with spherical precipitates of τ phase on it and interdendritic eutectic, as is shown in Fig. 3(a–c).

The microstructure observed in wedge shaped ingots for Mg-additions of 20, 30, 35 and 40at.% are shown in Fig. 4. The microstructures in Al–5.3at.%Zn–20at.%Mg alloy showed the presence of α-Al and the τ phase in form of dendrites in the three regions of ingot, Fig. 4(a–c). As the Mg content increases to 30at.%, the observed microstructures in all the ingot consisted of eutectic (α+τ) with crystals of the approximant τ for the Al–Zn–Mg icosahedral quasicrystal in the center of ingot and tip region, Fig. 4(d–f).

When the Mg content increases to 35at.%, Fig. 4(g–i), it was observed on tip region of the ingot, the presence of the approx-

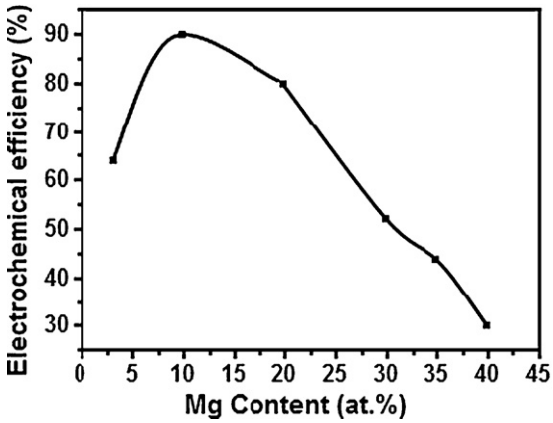

Fig. 8. Electrochemical efficiency as a function of Mg content.

imant to quasicrystal. In center and top regions of ingot, the presence of β phase was detected with some crystals of the approximant to quasicrystal and when the Mg content increases to 40at.%, the microstructure consisted mainly of β dendrites, Fig. 4(j–l).

Fig. 5(a) shows the X-ray diffraction pattern of Al–5.3at.%Zn–35at.%Mg obtained in the tip of ingot, as can be observed the peaks lying between 35 and 45 of 2θ are the main peaks which are identified as the approximant to quasicrystal phase Bergman $(Al,Zn)_{49}$ Mg_{32} classified as 1/1 cubic approximant [12,13], in (b) the β phase is observed in the center of the ingot at 2θ, 37.1; 38.6; 42.9; 61.9 and 76.

Fig. 6shows the different morphologies of the approximant, which consist of a nucleus from which dendrite arms start to grow. Electron diffraction patterns taken in Fig. 6(a–c) showed a two, three and five fold arrangements, respectively of this approximant.

Fig. 7shows a resume of characteristic microstructures and the distribution of the phases present in the three different zones obtained in wedge shaped ingots for the alloys under study.

3.2. Electrochemical efficiency

Fig. 8shows the electrochemical efficiency as a function of magnesium content. The international norms specified that an Al-anode should have a close-circuit potential active to −1.0 V, and an electrochemical efficiency, ε, between 2300 and 2700 Ah/kg [6].

Experimentally as can be observed, the electrochemical efficiency start increasing as the Mg-content increased from 3 to 10at.%. However, as the Mg-content continues increasing the electrochemical efficiency decreased reaching a minimum of 30%. The results indicated that the alloy Al–5.3at%Zn–10at.%Mg shows a maximum electrochemical efficiency of 90%, which indicates that this alloy composition can be used as sacrificial anode for cathodic protection of steel pipes or structure in sea water. This maximum electrochemical efficiency is reached because a fine distribution of τ-intermetallic precipitates was obtained in the α-Al matrix which promotes a good surface activation of the anode avoiding the formation of the protective oxide film on the alloy surface [14].

4. Conclusions

Microstructural characterization of Al–5.3at.%Zn alloy with additions of Mg casted in wedge shaped copper mould showed different morphology depending on cooling rate and Mg content. At a cooling rate of 20 K/s during solidification, α-Al and τ are the initial phases to form in Al–5.3at.%Zn–3at.%Mg and Al–5.3at.%Zn–10at.%Mg alloys.

The approximant $(Al,Zn)_{49}$ Mg_{32} for the Al–Zn–Mg icosahedral quasicrystal was formed at cooling rates of 50 and 150 K/s in ingots containing 30 and 35at.%Mg; while at 40at.%Mg content the β phase was formed in the same cooling rates. In addition, the alloy Al–5.3at%Zn–10at.%Mg with a microstructure constituted by dendrites of α-Al solid solution with spherical precipitates of τ phase on it and interdendritic eutectic showed a maximum electrochemical efficiency up to 90% with a potential application as Al-sacrificial anodes.

Acknowledgments

The authors acknowledge the financial support from PAPIT-UNAM: In 200808 project. We also thank to O- Novelo, A. Tejeda-Cruz and G. Aramburo for their technical support.

References

[1] G. Eger, Int. Z. Metallogr. 4 (1913) 50–128.
[2] J. Lendvai, Mat. Sci. Forum 217–222 (1996) 43–56.
[3] X.J. Jiang, B. Noble, B. Holme, G. Waterloo, J. Tafto, Metall. Mater. Trans. A31 (2000) 339–348.
[4] W.R. Osorio, C. Marina, A. Garcia, J. Alloys Compd. 397 (2005) 179–191.
[5] J.F. Li, C.X. Li, Z.W. Peng, W.J. Chen, Z.Q. Zheng, J. Alloys Compd. 460 (2008) 688–693.
[6] J. Genesca, J. Juarez-Islas, Contrib. Sci. 1 (3) (2000) 331–343.
[7] C. Gonzalez, O. Alvarez, J. Genesca, J.A. Juárez-Islas, Metall. Mater. Trans. A34 (2003) 2991–2997.
[8] O. Alvarez, C. Gonzalez, G. Aramburo, R. Herrera, J.A. Juarez Islas, Mater. Sci. Eng. A402 (2005) 320–324.
[9] M.A. Suarez, F.M. Sánchez-Arévalo, O. Alvarez, J. Colin, J.A. Juarez-Islas, Mater. Charact. 60 (2009) 420–424.
[10] J. Soto, G. Aramburo, C. Gonzalez, J. Genesca, R. Herrera, J.A. Juarez-Islas, Mater. Sci. Eng. A408 (2005) 303–308.
[11] D.A. Petrov, in: G. Petzow, G.E. Effenberg (Eds.), Ternary Alloys, vol.3, VCH, Weinheim, Germany, 1986, p. 57.
[12] A.I. Goldman, R.F. Kelton, Rev. Mod. Phys. 65 (1) (1993) 213–230.
[13] G. Bergman, J.L.T. Waugh, L. Pauling, Acta Crystallogr. 10 (1957) 254–259.
[14] D.R. Salinas, S.G. Garcia, J.B. Bessone, J. Appl. Electrochem. 29 (1999) 1063–1071.